Crystal Structure and Physical Properties of the New Selenide−Tellurides $Ba_3Cu_{17-x}(Se,Te)_{11}$

Bryan Kuropatwa, Yanjie Cui, Abdeljalil Assoud, and Holger Kleinke*

Department of Chemistry, University of Waterloo, Waterloo, ON, Canada N2L 3G1

Received August 26, 2008. Revised Manuscript Received November 14, 2008

The selenide−tellurides $Ba_3Cu_{17-x}(Se,Te)_{11}$ were synthesized from the elements in stoichiometric ratios at 750 °C, followed by slow cooling. $Ba_3Cu_{17-x}(Se,Te)_{11}$ adopts a new structure type, space group $R\bar{3}m$, with lattice dimensions of $a = 12.1718(4)$ Å, $c = 28.197(2)$ Å, $V = 3617.8(3)$ Å^3, for $Ba_3Cu_{14.4(2)}Se_{8.6(1)}Te_{2.4}$ ($Z = 6$). Noticeable variations both in the copper content (e.g., $2.0 \le x \le 2.6$) and Se:Te ratio (at least between 8.6:2.4 and 7.7:3.3) were observed, depending on the starting element ratios. All Cu atoms are tetrahedrally coordinated by Se and Te atoms and form a three-dimensional network via various Cu−Cu interactions. Because all Cu sites exhibit deficiencies, Ag ions can replace significant amounts of Cu under ambient conditions, proving a certain degree of ion conductivity. A small band gap was calculated for the electron precise material with $x = 1$, namely for the model $Ba_3Cu_{16}Se_8Te_3$. Accordingly, the materials with $x > 1$ are *p*-doped semiconductors, as confirmed via Seebeck and electrical conductivity measurements.

Introduction

Our ongoing investigations into barium copper chalcogenides and barium silver chalcogenides were originally motivated by the thermoelectric energy conversion.[1−3] Earlier reports about the thermoelectric properties of such materials were on the tellurides $BaCu_2Te_2$[4] and $A_2BaCu_8Te_{10}$ (A = K, Rb, Cs).[5] Recently, we uncovered several new materials, most of which form a new structure type with various Cu/Ag−Cu/Ag d^{10}−d^{10} interactions. Our first example of a new structure type in this family was $Ba_3Cu_2Sn_3Se_{10}$ with a [3 + 1] coordination of the Cu atoms and a Cu−Cu bond of 2.65 Å;[6] the second was $Ba_3Cu_{14-x}Te_{12}$ with almost planar $CuTe_3$ units, Cu−Cu bonds as short as 2.59 Å, Te_2^{2-} dumbbells, and extraordinarily low thermal conductivity;[7] the third $Ba_{6.76}Cu_{2.42}Te_{14}$ with bent Te_3^{2-} units;[8] and the fourth was $Ba_2Ag_4Se_5$ and its Cu-substituted variants with a unique linear Se_3^{4-} unit.[9] In the latter, the Cu/Ag substitution is limited, whereas a complete Cu/Ag substitution is possible in $BaAg_2Te_2$.[10]

Currently, we are expanding the chalcogenides under investigation, using two different chalcogen atoms (e.g., Se and Te). We thereby are applying the concept of anionic DFSO materials, which led to the discovery of several new materials in this decade. Originally, the concept of differential fractional site occupancies, DFSO, was utilized to create new structure types by mixing similar transition metal atoms (e.g., Nb and Ta) on one crystallographic site.[11,12] The DFSO concept thus led to the formation of the new materials $Nb_{1.72}Ta_{3.28}S_2$,[13] $Nb_{0.95}Ta_{1.05}S$,[14] $Nb_{4.92}Ta_{6.08}S_4$,[15] and $Nb_{6.74}Ta_{5.26}S_4$.[16] This concept was then successfully expanded to include mixtures on the anionic sites.[17,18] Recent examples of selenide−tellurides that exist only when both Se and Te are incorporated include $Ta_{15}Si_2Se_yTe_{10-y}$[19] and $LnSeTe_2$ (where Ln is a lanthanoid).[20] Partial replacement of Te with Se in tellurides[21] or vice versa (Se with Te in selenides)[22] may have a profound impact on the physical properties. Here, we report on the first barium copper selenide−tellurides, which are stabilized by—and evidently require—mixed Se/Te occupancies.

* To whom correspondence should be addressed. E-mail: kleinke@uwaterloo.ca.

(1) Tritt, T. M. *Science* **1995**, *272*, 1276–1277.
(2) DiSalvo, F. J. *Science* **1999**, *285*, 703–706.
(3) Rowe, D. M., *Thermoelectrics Handbook: Macro to Nano*; CRC Press, Taylor & Francis Group: Boca Raton, FL, 2006.
(4) Wang, Y. C.; DiSalvo, F. J. *J. Solid-State Chem.* **2001**, *156*, 44–50.
(5) Patschke, R.; Zhang, X.; Singh, D.; Schindler, J.; Kannewurf, C. R.; Lowhorn, N.; Tritt, T.; Nolas, G. S.; Kanatzidis, M. G. *Chem. Mater.* **2001**, *13*, 613–621.
(6) Assoud, A.; Soheilnia, N.; Kleinke, H. *Chem. Mater.* **2005**, *17*, 2255–2261.
(7) Assoud, A.; Thomas, S.; Sutherland, B.; Zhang, H.; Tritt, T. M.; Kleinke, H. *Chem. Mater.* **2006**, *18*, 3866–3872.
(8) Cui, Y.; Assoud, A.; Xu, J.; Kleinke, H. *Inorg. Chem.* **2007**, *46*, 1215–1221.
(9) Assoud, A.; Xu, J.; Kleinke, H. *Inorg. Chem.* **2007**, *46*, 9906–9911.
(10) Assoud, A.; Cui, Y.; Thomas, S.; Sutherland, B.; Kleinke, H. *J. Solid-State Chem.* **2008**, *181*, 2024–2030.
(11) Yao, X.; Marking, G.; Franzen, H. F. *Ber. Bunsen.* **1992**, *96*, 1552–1557.
(12) Köckerling, M.; Franzen, H. F. *Croat. Chem. Acta* **1995**, *68*, 709–719.
(13) Yao, X.; Franzen, H. F. *J. Am. Chem. Soc.* **1991**, *113*, 1426–1427.
(14) Yao, X.; Miller, G. J.; Franzen, H. F. *J. Alloys Compd.* **1992**, *183*, 7–17.
(15) Yao, X.; Franzen, H. F. *J. Solid-State Chem.* **1990**, *86*, 88–93.
(16) Yao, X.; Franzen, H. F. *Z. Anorg. Allg. Chem.* **1991**, *598−599*, 353–362.
(17) Kleinke, H. *Trends Inorg. Chem.* **2001**, *7*, 135–149.
(18) Kleinke, H. *J. Alloys Compd.* **2002**, *336*, 132–137.
(19) Debus, S.; Harbrecht, B. *Z. Anorg. Allg. Chem.* **2001**, *627*, 431–438.
(20) Tsinde, B. P. F.; Doert, T. *Solid-State Sci.* **2005**, *7*, 573–587.
(21) Huang, Z.; Bensch, W.; Mankovsky, S.; Polesya, S.; Ebert, H.; Kremer, R. K. *J. Solid-State Chem.* **2006**, *179*, 2067–2078.
(22) Assoud, A.; Soheilnia, N.; Kleinke, H. *Chem. Mater.* **2005**, *17*, 4509–4513.

10.1021/cm802304k CCC: $40.75
Published on Web 12/11/2008

Experimental Section

Synthesis. All reactions commenced from the elements (Ba: 99% nominal purity, pieces, Aldrich; Cu: 99.5%, −150 mesh powder; Alfa Aesar; Se: 99.99%, pellets <4 mm in diameter, Aldrich; Te: 99.8%, −200 mesh powder, Aldrich), with sample masses of ∼600 mg. The elements were stored and handled in a glovebox filled with argon. Inside that box, the elements were placed into fused silica tubes, which were subsequently sealed under vacuum (10^{-3} mbar). The tubes were then heated in a resistance furnace at 750 °C for 12 h. Thereafter, the furnace was slowly cooled to 450 °C over a period of 200 h to allow for crystallization. Lastly, the furnace was switched off to prompt rapid cooling.

The black title compound was first encountered in a reaction with the Ba:Cu:Se:Te ratio of 2:3:2:1, and identified as $Ba_3Cu_{14.4}Se_{8.6}Te_{2.4}$ via the single-crystal structure determination described below. Because its structure contained Cu-deficient sites and mixed Se/Te occupancies, several reactions were loaded to analyze the phase range of $Ba_3Cu_{17-x}Se_{11-y}Te_y$, with $x = 0$, 0.5, 1.0, 1.6, 2.0, 2.5, 2.7, and 3 and $y = 0$, 1, 2, 2.5, 3, 4, 5, and 6.

All samples were analyzed by means of powder X-ray diffraction (XRD), utilizing the INEL diffractometer with Cu $K\alpha_1$ radiation. Apparently phase-pure samples were obtained only with $2 \leq x \leq 2.7$ and $1 \leq y \leq 3$. In the other cases, the identified side products were mostly copper chalcogenides. A differential scanning calorimetry (DSC) measurement (using a Netzsch Model STA 409PC Luxx, as described earlier[6,23]) revealed the melting point of $Ba_3Cu_{14.4}Se_{8.5}Te_{3.5}$ to be ∼695 °C.

Analysis. To further prove, in principle, the existence of a phase width, as well as the absence of heteroelements such as silicon stemming from the reaction container, several samples of different starting compositions were analyzed via energy-dispersive X-ray analysis (EDX), using an electron microscope (LEO, Model 1530) with an additional EDX device (EDAX Pegasus 1200). The scans were performed with an acceleration voltage of 20 kV under high dynamic vacuum. No heteroelements were detected in any case. Although the copper content did not change significantly from one sample to another, the Se:Te ratio of different samples varied from ∼14:1 to 3:1. This corresponds to $0.8 < y < 3.7$ in $Ba_3Cu_{17-x}Se_{11-y}Te_y$, which is comparable to the range of y deduced from the powder XRD diagrams ($1 \leq y \leq 3$). Although the EDX analysis is known to be only semiquantitative, this large range indicates a significant phase width.

Structure Determination. The first X-ray single-crystal structure study (I) was performed on a platelike single crystal of the reaction with the starting ratio of 2Ba:3Cu:2Se:1Te. A Bruker Smart APEX CCD diffractometer with graphite-monochromatized Mo $K\alpha_1$ radiation was used for the data collection, performed by scans of 0.3° in ω in two groups of 606 frames (each with an exposure time of 60 s) at $\phi = 0°$ and 90°. The data were corrected for Lorentz and polarization effects. Absorption corrections were based on fitting a function to the empirical transmission surface as sampled by multiple equivalent measurements using SADABS incorporated into the computer package SAINT.[24]

The structure solution and refinements were performed with the SHELXTL program package.[25] The lattice parameters indicated rhombohedral symmetry. No systematic absences were identified, leaving $R\bar{3}m$ as the space group of highest symmetry. Using the "Direct Methods of SHELXS" gave 12 atomic sites, to which one Ba, two Te, three Se, and six Cu atoms were assigned, based on their interatomic distances and relative heights. Subsequent refinements revealed large thermal expansion parameters in case of one Te and two Cu sites, pointing toward Se/Te mixtures and Cu deficiencies, respectively. As a consequence, the occupancies of all Cu sites were refined, yielding occupancies between 0.55 and 0.96. Similarly, all chalcogen sites (Q) were refined as being mixed albeit fully occupied by Se and Te, allowing the Se:Te ratio to vary freely. Of the five Q sites, one was occupied solely by Te (i.e., within its standard deviation of 2%), denoted as Te1, two were occupied by Se (Se3 and Se5), one was occupied by (Q2), which was clearly mixed occupied (54% Se, 46% Te), and the fifth (Q4) seemed to be a Se site with a small amount of Te, namely, 7%. In the final refinement, Te1 was fixed as a Te site and Se3 and Se5 as Se sites. This refinement yielded the formula of $Ba_3Cu_{14.4(2)}Se_{8.6(1)}Te_{2.4}$. To investigate the possibility of additional long-range Se/Te or Cu ordering, additional refinements were performed at lower symmetry, in accordance with the allowed space groups, i.e., $R3m$, $R32$, and $R\bar{3}$. Because none of the latter models constituted an improvement in the residual values or showed tendency to additional ordering, the space group of highest symmetry, $R\bar{3}m$, was selected as the final model.

To prove the existence of a phase range, three more crystals were analyzed using the Smart APEX CCD diffractometer. Their nominal compositions were "$Ba_3Cu_{15}Se_7Te_4$" (case II), "$Ba_3Cu_{14.5}Se_8Te_3$" (case III), and "$Ba_3Cu_{15}Se_{10}Te$" (case IV), i.e., the first was more selenium-poor and the last was more selenium-rich. In case II, the formula was refined to $Ba_3Cu_{15.0(1)}Se_{7.75(6)}Te_{3.25}$, with more tellurium on the Q2 site (74%) and comparable Cu occupancies between 56% and 96%. Case II has the highest tellurium content and, therefore, the largest unit cell volume of 3665.8(2) Å^3, which constitutes an increase of 1.3% from case I. Case III is intermediate in tellurium content, with $V = 3629.9(3)$ Å^3 and the refined formula being $Ba_3Cu_{14.4(2)}Se_{8.30(8)}Te_{2.70}$. In case IV, the crystal quality was not sufficient to refine the occupancies, but the 3.1% decrease in the unit cell volume from 3617.8(3) Å^3 (case I) to 3504.8(2) Å^3 (case IV) implies a significantly higher selenium content. The crystallographic data are summarized in Table 1, and the atomic parameters including the occupancy factors are summarized in Table 2.

Ion-Exchange Reactions. Motivated by the three-dimensional network of deficient Cu atom sites, we attempted to replace some of the Cu atoms with Ag atoms at room temperature. Finely crushed microcrystalline samples of nominal composition $Ba_3Cu_{14.4}Se_{8.5}Te_{2.5}$ and $Ba_3Cu_{15}Se_{10}Te$ were placed in glass vials in respective masses of 45 and 40 mg. To each vial, ∼10 drops of 2N $AgNO_3$ solution were added via a glass pipet. The vials were capped and placed in a cool, dark enclosure for approximately 2−3 weeks, while the vials were lightly stirred on a day-to-day basis. The mixtures began to turn blue after a few hours, indicating the presence of Cu^{2+} ions in the solutions. The chalcogenides did not dissolve into the solution. Afterward, the powders were filtered and dried in an evaporating dish overnight. EDX analyses revealed significant presence of silver in the crystals of both samples, of ∼7%−10% of the copper content. Also, the powder XRD diagrams revealed a slight shift toward smaller angles, which is indicative of a unit cell increase caused by partial substitution of small Cu atoms by larger Ag atoms. An additional single-crystal structure study of the selenium-rich sample revealed a volume increase of 2% (from $a = 12.0096(3)$ Å, $c = 28.059(2)$ Å, and $V = 3504.8(2)$ Å^3 to $a = 12.0952(2)$ Å, $c = 28.2032(9)$ Å, and $V = 3573.2(1)$ Å^3).

Calculation of the Electronic Structure. We utilized the LMTO (linear muffin tin orbitals) method with the atomic spheres

(23) Lee, C.-S.; Kleinke, K. M.; Kleinke, H. *Solid-State Sci.* **2005**, *7*, 1049–1054.
(24) *SAINT. Version 4 ed.*; Siemens Analytical X-ray Instruments, Inc.: Madison, WI, 1995.
(25) Sheldrick, G. M., *SHELXTL, Version 5.12 ed.*; Siemens Analytical X-Ray Systems: Madison, WI, 1995.

Table 1. Crystallographic Data for $Ba_3Cu_{17-x}(Se,Te)_{11}$

property	$Ba_3Cu_{14.4(2)}Se_{8.6(1)}Te_{2.4}$	$Ba_3Cu_{14.4(2)}Se_{8.30(8)}Te_{2.70}$	$Ba_3Cu_{15.0(1)}Se_{7.75(6)}Te_{3.25}$
formula weight	2311.74 g/mol	2325.38 g/mol	2396.09 g/mol
measurement temperature, T	298(2) K	298(2) K	298(2) K
λ	0.71073 Å	0.71073 Å	0.71073 Å
space group	$R\bar{3}m$	$R\bar{3}m$	$R\bar{3}m$
lattice parameters			
a	12.1718(4) Å	12.1897(3) Å	12.2339(3) Å
c	28.197(2) Å	28.2087(17) Å	28.2819(16) Å
V	3617.8(3) Å^3	3629.9(3) Å^3	3665.8(2) Å^3
Z	6	6	6
μ	32.956 mm^{-1}	32.786 mm^{-1}	32.854 mm^{-1}
calculated density, ρ_{calcd}	6.366 g/cm^3	6.383 g/cm^3	6.512 g/cm^3
$R(F_o)^a/R_w(F_o^2)^b$	0.064/0.126	0.046/0.091	0.038/0.087

^{a} $R(F_o) = \sum F_o - F_c/\sum F_o$ ^{b} $R_w(F_o^2) = \{\sum[w(F_o^2 - F_c^2)^2]/\sum[w(F_o^2)^2]\}^{1/2}$

Table 2. Atomic Coordinates, Equivalent Isotropic Displacement Parameters, and Occupancy Factors of $Ba_3Cu_{15.0}Se_{7.75}Te_{3.25}$ (Case II)

						Occupancy		
atom	site	x	y	z	U_{eq} (Å^2)	case II	case I^a	case III^b
Ba	18h	0.47585(3)	0.52415(3)	0.08605(2)	0.0158(2)	1	1	1
Te1	18h	0.77678(3)	0.22322(3)	0.11263(2)	0.0126(2)	0.74(1)	0.46(2)	0.56(2)
Se1	18h	0.77678(3)	0.22322(3)	0.11263(2)	0.0126(2)	0.26(1)	0.54(2)	0.44(2)
Te2	6c	0	0	0.08002(5)	0.0191(3)	1	1	1
Se3	18f	0.31700(8)	0	0	0.0124(2)	1	1	1
Se4	6c	0	0	0.35749(6)	0.0152(6)	0.96(2)	0.93(4)	0.97(3)
Te4	6c	0	0	0.35749(6)	0.0152(6)	0.04(2)	0.07(4)	0.03(3)
Se5	18h	0.47441(5)	0.52559(5)	0.20499(3)	0.0141(2)	1	1	1
Cu1	36i	0.2256(2)	0.0124(1)	0.13570(5)	0.0391(5)	0.909(6)	0.817(11)	0.834(8)
Cu2	18h	0.43219(8)	0.56781(9)	0.34939(7)	0.0374(7)	0.949(8)	0.96(2)	0.96(1)
Cu3	18h	0.53054(8)	0.46946(8)	0.27982(5)	0.0242(5)	0.957(8)	0.95(1)	0.930(9)
Cu4	18h	0.54981(11)	0.45019(11)	0.38259(9)	0.0399(8)	0.874(9)	0.84(2)	0.84(1)
Cu5	6c	0	0	0.16876(19)	0.040(2)	0.56(2)	0.55(3)	0.55(2)
Cu6	6c	0	0	0.26646(14)	0.028(1)	0.67(1)	0.64(2)	0.65(2)

^{a} $Ba_3Cu_{14.4}Se_{8.6}Te_{2.4}$ (I). ^{b} $Ba_3Cu_{14.4}Se_{8.3}Te_{2.7}$ (III).

approximation (ASA) for the electronic structure calculations.[26,27] Therein, density functional theory is applied with the local density approximation (LDA) to treat correlation effects.[28] The following wave functions were used: for Ba 6*s*, 6*p* (downfolded[29]), 5*d* and 4*f*; for Cu 4*s*, 4*p*, and *3*d, for Se *4*s, 4*p*, and 4*d* (downfolded), and for Te 5*s*, 5*p*, and 5*d* and 4*f* (the latter two downfolded). The eigenvalue problem was solved on the basis of 126 *k*-points that were chosen with an improved tetrahedron method.[30] Crystal orbital Hamilton populations[31] were calculated to gain insight into the strength of the Cu−Cu interactions.

The structural parameters were taken from the refinement on $Ba_3Cu_{15.0}Se_{7.75}Te_{3.25}$. The Cu sites with occupancies of >87% were treated as fully occupied, and one of the two Cu5 sites (refined occupancy: 56%) and one of the two Cu6 sites (67%) per primitive cell was removed. The two mixed Se/Te sites were treated as follows: the six Q1 atoms per primitive cell with 74% Te as four Te and two Se, and Q4 with 96% Se as a Se site. As a result, the model has the formula $Ba_3Cu_{16}Se_8Te_3$ in space group *Cm*.

Physical Property Measurements. A cold-pressed bar with dimensions of 6 mm × 1 mm × 1 mm of the sample $Ba_3Cu_{14.4}Se_{8.5}Te_{2.5}$ was used for Seebeck coefficient (*S*) and electrical conductivity measurements, after applying silver paint (Ted Pella) to create the electric contacts. For the former, a commercial thermopower measurement apparatus (MMR Technologies) was used, measuring the value of *S* under dynamic vacuum in the temperature range of 300−550 K with constantan as an internal standard, to determine the temperature difference. The specific electrical conductivity (σ) was determined via a four-point-method, using a homemade device between 320 K and 180 K. The achieved density was ~80% of the theoretical maximum determined via the single-crystal structure study. The resistances (*R*) were calculated from the voltage drops using Ohm's law, i.e., $R = \Delta V/I$, where *I* is the current. σ(T) was calculated after measuring the lengths between the contacts (*L*), according to $\sigma = L/(AR)$, with the area *A* being defined as having dimensions of 1 mm × 1 mm.

Results and Discussion

Crystal Structure. The crystal structure of $Ba_3Cu_{17-x}(Se,Te)_{11}$ is comprised of a three-dimensional network of corner-, edge-, and face-sharing CuQ_4 tetrahedra. Because no short Q−Q contacts occur in this structure, the oxidation states may be readily assigned to Ba^{2+}, Cu^{1+}, and Q^{2-}. Accordingly, the chalcogenides with $x = 1$, i.e., $Ba_3Cu_{16}(Se,Te)_{11}$, are electron precise. Figure 1 shows the crystal structure with the Cu_{26} clusters in polyhedral representation.

A multitude of Cu−Cu contacts occur between 2.53 Å and 2.94 Å (Table 3). Similar distances were found in $Ba_3Cu_{14-x}Te_{12}$,[7] noting that these closed-shell (d^{10}−d^{10}) interactions occur regularly in copper chalcogenides, and are usually bonding as a consequence of the hybridization of the filled *d* states with the nominally empty, energetically higher lying *s* and *p* orbitals.[32−34] The Cu_{26} clusters are

(26) Andersen, O. K. *Phys. Rev. B* **1975**, *12*, 3060–3083.
(27) Skriver, H. L., *The LMTO Method*; Springer: Berlin, Germany, 1984.
(28) Hedin, L.; Lundqvist, B. I. *J. Phys. C* **1971**, *4*, 2064–2083.
(29) Lambrecht, W. R. L.; Andersen, O. K. *Phys. Rev. B* **1986**, *34*, 2439–2449.
(30) Blöchl, P. E.; Jepsen, O.; Andersen, O. K. *Phys. Rev. B* **1994**, *49*, 16223–16233.
(31) Dronskowski, R.; Blöchl, P. E. *J. Phys. Chem.* **1993**, *97*, 8617–8624.
(32) Mehrotra, P. K.; Hoffmann, R. *Inorg. Chem.* **1978**, *17*, 2187–2189.

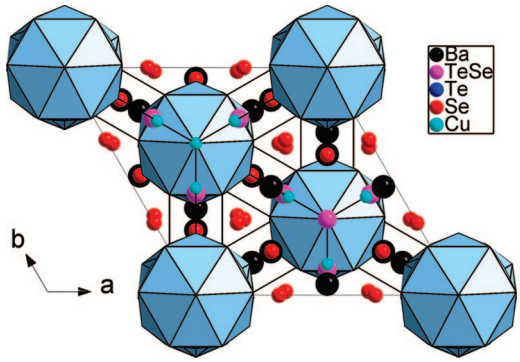

Figure 1. Crystal structure of $Ba_3Cu_{17-x}(Se,Te)_{11}$; the Cu_{26} polyhedra are emphasized.

Table 3. Selected Interatomic Distances [Å] of $Ba_3Cu_{17-x}(Se,Te)_{11}$

	Interatomic Distance, *d* (Å)	
interaction	$Ba_3Cu_{14.4(2)}Se_{8.6(1)}Te_{2.4}$	$Ba_3Cu_{15.0(1)}Se_{7.75(6)}Te_{3.25}$
Ba−Se5	3.251(2) ×2	3.233(1) ×2
Ba−Se3	3.328(2) ×2	3.346(1) ×2
Ba−Se5	3.337(2)	3.364(1)
Ba-Q4	3.487(4)	3.491(2)
Ba-Q1	3.567(3) ×2	3.595(1) ×2
Cu1−Se5	2.303(3)	2.336(2)
Cu1−Cu1	2.417(6)	2.457(3)
Cu1-Q1	2.674(3)	2.701(2)
Cu1-Q1	2.684(4)	2.722(2)
Cu1−Cu4	2.746(5)	2.738(3)
Cu1−Cu1	2.787(8)	2.813(2)
Cu1−Cu3	2.840(4)	2.846(2)
Cu1−Cu5	2.864(6)	2.877(3)
Cu1−Cu1	2.968(8)	2.912(3)
Cu1−Te2	3.135(4)	3.115(2)
Cu2−Q4	2.378(4)	2.383(2)
Cu2−Cu6	2.527(6)	2.540(3)
Cu2−Se3	2.559(2) ×2	2.561(1) ×2
Cu2−Cu4	2.645(5)	2.663(3)
Cu2−Q1	2.694(4)	2.742(2)
Cu2−Cu3	2.885(5)	2.866(3)
Cu3−Se3	2.497(2) ×2	2.505(1) ×2
Cu3−Cu4	2.690(2) ×2	2.706(1) ×2
Cu3−Cu1	2.840(4) ×2	2.813(2) ×2
Cu3−Cu4	2.914(5)	2.935(3)
Cu3−Te2	2.960(3)	2.980(2)
Cu3−Se5	2.412(3)	2.428(2)
Cu3−Cu2	2.885(5)	2.866(3)
Cu4−Se3	2.535(3) ×2	2.545(2) ×2
Cu4−Te2	2.613(4)	2.624(2)
Cu4−Cu3	2.690(3) ×2	2.706(1) ×2
Cu4−Cu1	2.746(5) ×2	2.738(3) ×2
Cu4-Q1	2.870(6)	2.880(3)
Cu4−Cu3	2.914(5)	2.935(3)
Cu4−Cu2	2.645(5)	2.663(3)
Cu5−Cu6	2.662(14)	2.763(7)
Cu5−Q1	2.718(6) ×3	2.757(3) ×3
Cu5−Cu1	2.864(6) ×4	2.846(2) ×4
Cu5−Cu1	2.864(6) ×2	2.846(2) ×2
Cu5−Te2	2.559(12)	2.510(6)
Cu6−Cu2	2.527(6) ×3	2.540(3) ×3
Cu6−Q1	2.629(4) ×3	2.668(2) ×3
Cu6−Q4	2.605(8)	2.575(4)
Cu6−Cu5	2.662(14)	2.763(7)

comprised of hexagonal Cu_{12} antiprisms formed by the Cu1, Cu3, and Cu4 atoms. One hexagonal face of the antiprisms

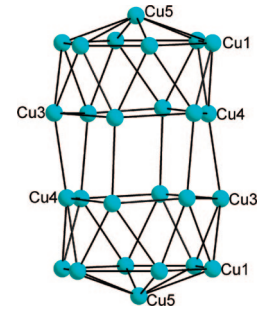

Figure 2. The Cu_{26} cluster of $Ba_3Cu_{17-x}(Se,Te)_{11}$.

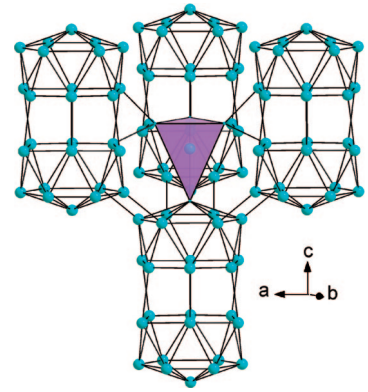

Figure 3. The three-dimensional network of Cu atoms, with an emphasis on the $Cu6Cu_4$ tetrahedron connecting the Cu_{26} clusters of $Ba_3Cu_{17-x}(Se,Te)_{11}$.

is capped by the Cu5 atom, and the Cu atoms of the second hexagonal face form bonds with a second symmetry-equivalent Cu_{12} antiprism (see Figure 2).

As emphasized in Figure 3, the Cu network is three-dimensional, with the Cu_{26} clusters being connected to the surrounding Cu_{26} clusters via additional Cu−Cu contacts smaller than 3 Å of the intercluster atoms Cu2 and Cu6. The Cu6 atom, situated in the center of a tetrahedron, is connecting four Cu_{26} clusters together through three intercluster atoms (Cu2) and one cluster atom (Cu5). Considering the three-dimensional extension of the Cu−Cu contacts in combination with the Cu deficiencies on all sites (ranging from 4% to 45%), the possibility of Cu ion conductivity seems to be high. On the other hand, the anisotropic displacement parameters are mostly (but not completely) inconspicuous, in contrast to the best Cu ion conductors such as $Rb_4Cu_{16}I_7Cl_{13}$[35,36] and Cu_6PS_5Cl.[37]

To probe the Cu ion mobility, ion-exchange reactions were performed in an $AgNO_3$ solution. Because a few days passed until the blue color—which was caused by Cu cations in the solution—became evident, the ion conductivity is very slow. For comparison, the process was much slower than the Ag exchange experiment on $Cu_2P_3I_2$.[38] However, the ion con-

(33) Merz Jr, K. M.; Hoffmann, R. *Inorg. Chem.* **1988**, *27*, 2120–2127.
(34) Pyykkö, P. *Chem. Rev.* **1997**, *97*, 597–636.
(35) Owens, B. B. *J. Power Source* **2000**, *90*, 2–8.
(36) Kanno, R.; Ohno, K.; Kawamoto, Y.; Takeda, Y.; Yamamoto, O.; Kamiyama, T.; Asano, H.; Izumi, F.; Kondo, S. *J. Solid-State Chem.* **1993**, *102*, 79–92.
(37) Gagor, A.; Pietraszko, A.; Kaynts, D. *J. Solid-State Chem.* **2008**, *181*, 777–782.
(38) Möller, M. H.; Jeitschko, W. *J. Solid State Chem.* **1986**, *65*, 178–189.

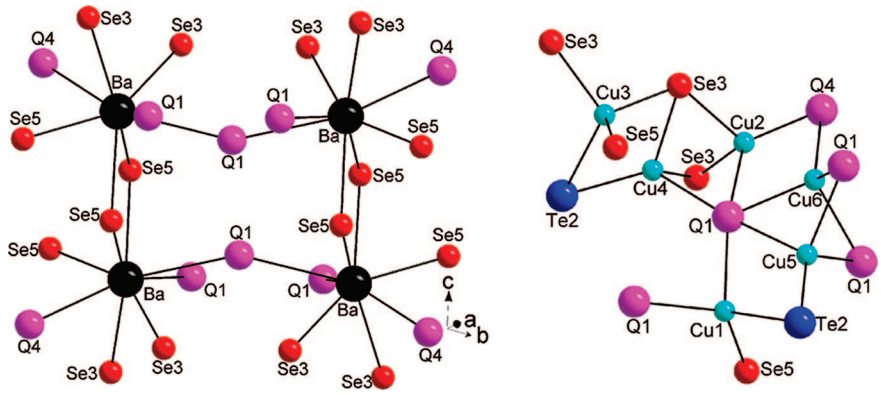

Figure 4. A section of the Ba−Q (left) and Cu−Q (right) network of $Ba_3Cu_{17-x}(Se,Te)_{11}$.

ductivity observed here is significant, because Ag was able to replace 7%−10% of the Cu in the solid under ambient conditions without destroying the crystals, as detected via EDX analysis and proven by the unit-cell size increase.

The Ba cations are incorporated in bicapped trigonal prismatic voids, surrounded by three Se5 atoms in distances of 3.25−3.34 Å, two Se3 (3.33 Å), one Se4 (3.49 Å), and two Q1 (3.57 Å). Therefore, the Te2 site is the only chalcogen site with no direct contact to the Ba atom. The Ba−Q polyhedra extend themselves along all directions, similar to the CuQ_4 tetrahedra that share corners, edges, and faces (see Figure 4).

Concerning the Se/Te distribution, note that, of the five chalcogen sites, one is exclusively occupied by Te (Te2), three are almost entirely Se sites (Se3, Se5, and Q4 with at least 93% Se), and one (Q1) exhibits a larger range of Te contents, namely between 74% (in the case of $Ba_3Cu_{15.0}Se_{7.75}Te_{3.25}$) and 46% (in the case of $Ba_3Cu_{14.4}Se_{8.6}Te_{2.4}$). Hence, the variations in Te reflect themselves almost exclusively in different tellurium contents of Q1. The Te2 site is the one with the largest coordination sphere, being surrounded by 13 Cu atoms, and it is the only Q site without a Ba neighbor. The Q1 site is intermediate, surrounded by eight Cu and two Ba sites, whereas the (almost pure) Se sites (Se3, Q4, and Se5) are, respectively, only surrounded by six, four, and three Cu atoms as well as two, two, and three Ba atoms. These vast differences in the coordination environment of the Q atoms may be the reason why this structure was not found in either of the ternary systems (Ba/Cu/Se or Ba/Cu/Te).

Electronic Structure. The density of states (DOS) of the electron precise model $Ba_3Cu_{16}Se_8Te_3$ reveals a very small band gap of the order of 0.02 eV (see the left part of Figure 5). The area below the Fermi level (E_F) is predominated by Cu 3*d* states with contributions from the Se 4*p* and Te 5*p* states, and the conduction band consists of Ba *s*, Cu *s*, and Cu *p* states. With the phase width being within $Ba_3Cu_{15}(Se,Te)_{11}$ and $Ba_3Cu_{14.4}(Se,Te)_{11}$, all these chalcogenides exhibit a Cu deficiency and are heavily doped *p*-type semiconductors.

The Cu−Cu COHP curve, cumulated over all Cu−Cu bonds under 2.8 Å in length, provides evidence for the significance of these interactions (see the right part of Figure 5). Their integrated COHP values (ICOHP)[39−41] vary between −1.00 eV for the 2.46 Å bond and −0.44 eV for the 2.71 Å bond, and even the 2.94 Å bond exhibits the still significant ICOHP value of −0.28 eV. The Cu deficiencies observed in all cases thus far have only a minor impact onto the ICOHP values, because the Cu−Cu interactions show only minor contributions to the area directly below E_F, similar to the situation in $Ba_3Cu_{14-x}Te_{12}$.[7]

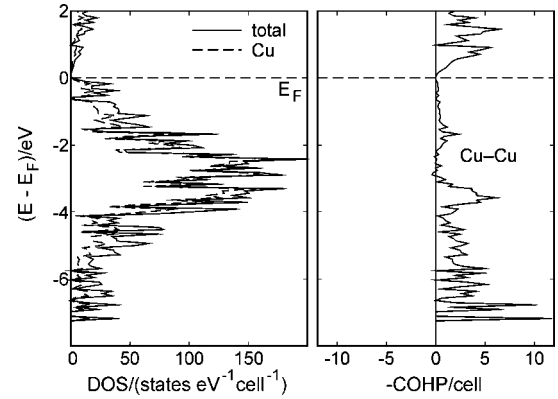

Figure 5. Density of states (DOS, left) and cumulated Cu−Cu COHP curve (right) of the $Ba_3Cu_{16}Se_8Te_3$ model.

Physical Properties. The electrical transport properties of $Ba_3Cu_{14.4}Se_{8.5}Te_{2.5}$ are depicted in Figure 6. Both the Seebeck coefficient and the electrical conductivity are typical for (*p*-type) semiconductors with high charge carrier concentration, as deduced from the electronic structure calculation on the $Ba_3Cu_{16}Se_8Te_3$ model: the Seebeck coefficient increases linearly from +50 μV/K at 300 K to +100 μV/K at 550 K. Other $Ba_3Cu_{17-x}(Se,Te)_{11}$ samples that we tested showed room-temperature Seebeck values between +40 μV/K and +75 μV/K, which covers a slightly higher range than in the case of $Ba_3Cu_{14-x}Te_{12}$ (S(300 K) between +35 μV/K and +50 μV/K).[7] The electrical conductivity of $Ba_3Cu_{14.4}Se_{8.5}Te_{2.5}$ increases from 98 Ω^{-1} cm^{-1} at 180 K to 130 Ω^{-1} cm^{-1} at 320 K, indicating that the charge carrier concentration does not significantly increase as the temperature increases. Here, note that the apparently small ionic

(39) Landrum, G. A.; Dronskowski, R. *Angew. Chem., Int. Ed.* **2000**, *39*, 1560–1585.
(40) Dashjav, E.; Kleinke, H. *J. Solid-State Chem.* **2003**, *176*, 329–337.
(41) Soheilnia, N.; Assoud, A.; Kleinke, H. *Inorg. Chem.* **2003**, *42*, 7319–7325.

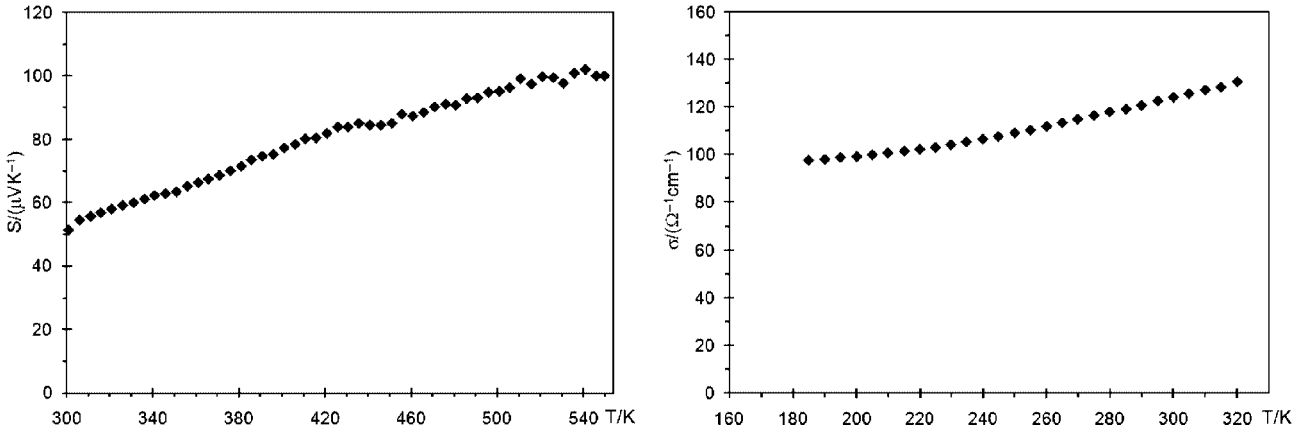

Figure 6. Seebeck coefficient (left) and electrical conductivity (right) of $Ba_3Cu_{14.4}Se_{8.5}Te_{2.5}$.

conductivity also contributes to the cross conductivity,[42] but its impact should be negligible.

Conclusions

A new structure type was uncovered and adopted by $Ba_3Cu_{17-x}(Se,Te)_{11}$. This structure apparently exists only when both selenium and tellurium are used. Although the Se:Te ratio may vary as determined via different single-crystal structure and EDX studies, one of the five chalcogen sites is always mixed occupied by Se and Te, while a second site is solely occupied by Te, with the remaining sites being almost exclusively Se positions. The large differences in the coordination spheres of the chalcogen sites are concluded to be responsible for the different occupancy ratios.

According to the electronic structure calculations, $Ba_3Cu_{17-x}(Se,Te)_{11}$ would be an intrinsic semiconductor when $x = 1$; however, the experiments indicate that $x > 2$. This is in agreement with $Ba_3Cu_{14.4}Se_{8.5}Te_{2.5}$ being classified as a heavily doped *p*-type semiconductor. The absolute numbers and temperature dependencies of the Seebeck coefficient and electrical conductivity are comparable to those of (also cold-pressed pellets of) $Mo_3Sb_{5.4}Te_{1.6}$[43] and $Re_3Ge_{0.6}As_{6.4}$,[44] which reach ZT values in the range of 0.3−1.0 at elevated temperatures.[45] Hypothetically, one might expect $Ba_3Cu_{14.4}Se_{8.5}Te_{2.5}$ to have higher ZT values, because of its likely lower thermal conductivity, as implicated, for example, by a comparison with the related $Ba_3Cu_{14-x}Te_{12}$.[7] However, the experimentally proven mobility of the Cu ions militates against the use of $Ba_3Cu_{17-x}(Se,Te)_{11}$ in a thermoelectric device, as such a device would deteriorate within days.

Acknowledgment. Financial support from NSERC, CFI, OIT (Ontario Distinguished Researcher Award for H.K.), and the Canada Research Chair program (CRC for H.K.) is appreciated.

Supporting Information Available: Three crystallographic information files (CIFs). This material is available free of charge via the Internet at http://pubs.acs.org.

CM802304K

(42) Ogawa, H.; Kobayashi, M. *Solid-State Ionics* **2002**, *148*, 211–217.
(43) Zhang, H.; He, J.; Zhang, B.; Su, Z.; Tritt, T. M.; Soheilnia, N.; Kleinke, H. *J. Electron. Mater.* **2007**, *36*, 727–731.
(44) Soheilnia, N.; Xu, H.; Zhang, H.; Tritt, T. M.; Swainson, I.; Kleinke, H. *Chem. Mater.* **2007**, *19*, 4063–4068.
(45) Xu, H.; Soheilnia, N.; Zhang, H.; Alboni, P. N.; Tritt, T. M.; Kleinke, H. *Mater. Res. Soc. Proc.* **2008**, *1044*, 459–467.